

# Experiments on Surface Waves Interacting with Flexible Aquatic Vegetation

Luca Cavallaro\*, Antonino Viviano, Giovanni Paratore, and Enrico Foti

*Department Civil Engineering and Architecture, University of Catania, Catania 95124, Italy*

Received 18 July 2017; Revised 27 November 2017; Accepted 11 April 2018

© KSO, KIOST and Springer 2018

**Abstract** – Surface wave interaction with aquatic vegetation appears to play a key role in coastal hydro-morpho-dynamics. As an example, the presence of a dense meadow at intermediate water depth is usually associated with a stable and resilient shore. Wave-meadow interactions are investigated here by means of physical modelling, with a focus on wave height distribution and hydrodynamics. The central part of a wave flume is covered by flexible artificial seagrass, composed of polyethylene leaves. This vegetation is tested in both near emergent and submerged conditions. The wave height reduction is evaluated by means of a drag coefficient defined from linear wave theory, which contains all the unknowns of the adopted methodology. The behaviour of such a coefficient is investigated as a function of a wave related Reynolds number. The influence of the flexibility of the leaves is also considered, together with a wave frequency parameter. The results show a complex behaviour with three different trends for near rigid, intermediate or highly flexible leaves. Amplitudes of the orbital velocities are investigated and show a fairly good match with the linear wave theory. On the contrary, the mean velocity along the water column appears to be modified by the seagrass for submerged leaves.

**Keywords** – water waves, vegetation, hydrodynamics

## 1. Introduction

Aquatic vegetation exerts important effects on the coastal ecosystem and hydrodynamics, especially in shallow waters where the length of the plants is similar to the water depth. Indeed, the aquatic vegetation has structural and functional consequences for the environment by producing flow resistance and modifying the flow locally (Carpenter and Lodge 1986; Bouma et al. 2005; Peralta et al. 2006). Seagrass meadows play a major role in maintaining biodiversity since they favor the growth of algae, fish and invertebrates. Seagrasses

play a relevant role in coastal protection since they increase bottom roughness, thus reducing near-bed velocity and modifying the sediment transport and increasing the wave attenuation. Furthermore, vegetation may exert an influence with regard to coastal hazards by altering the wave propagation on the beach (John et al. 2016) and the load on coastal structures (Lakshmanan et al. 2012).

However, the interaction between vegetation and flow has not been clearly defined up to now, especially when integrated into a wave propagation model.

Such an interaction is amplified in the presence of flexible plants since seagrass and waves affect each other in highly coupled, nonlinear ways (Koch et al. 2006). As a result of this interaction, seagrass represents a variable hydraulic roughness: as the flow velocity increases the leaves increasingly bend, until they eventually lie on the bottom. Therefore, the roughness has to be seen as a function of the flow conditions (velocity and depth of the marine current). Of course, the effects of such a roughness are especially marked in lagoons, characterized by large expanses with low water depths of the order of one meter. In the presence of waves, the flow becomes periodic and the leaves follow the movements of the flow, maintaining quite similar oscillatory movements. Under these conditions, the effects that the plants have on the flow become difficult to identify as regards, for example, vertical velocity distribution, turbulence and energy dissipation.

The interaction between rigid vegetation and waves was analyzed by Lowe et al. (2005), while Bradley and Houser (2009) focused their attention on the wave attenuation with flexible plants and wave motion, obtaining a significant wave height reduction. Results of such studies show that the wave height decay is well understood for submerged vegetation by adopting the exponential function proposed

\*Corresponding author. E-mail: [luca.cavallaro@dica.unict.it](mailto:luca.cavallaro@dica.unict.it)

by Kobayashi et al. (1993) and Mendez et al. (1999), in which all the unconsidered aspects are embedded in the drag coefficient  $C_D$ , which is used to quantify the resistance of an object in the fluid environment. Such a resistance is due to the skin friction on the surface of the kelp which could be affected by viscous, turbulent and inertia effects. Previous studies have tried to link  $C_D$  with the Reynolds number, which represents the ratio between turbulent and viscous forces, and the Keulegan-Carpenter number, which compares the horizontal water displacement under waves and the kelp dimension (see Kobayashi et al. 1993; Mendez et al. 1999; Mendez and Losada 2004; Bradley and Houser 2009; Cavallaro et al. 2010; Sanchez-Gonzalez et al. 2011; Koftis et al. 2013; Houser et al. 2015). The first coefficient allows for the taking into account of the importance of flow turbulence. The second coefficient instead is specifically used for analyzing the effect of wave motion on the kelp.

More recently, Luhar and Nepf (2011, 2016) analyzed the dynamics of flexible blades induced by waves in order to explain the high dispersion of experimental data with respect to the above-mentioned parameters. Furthermore, Houser et al. (2015) analyzed the influence of blade flexibility in the wave height attenuation over submerged meadows.

Several laboratory and field studies have been performed in order to estimate the flow induced by the waves inside a meadow (Bradley and Houser 2009; Luhar et al. 2010, 2013; Koftis et al. 2013). Such studies showed that a mean current is generated within a meadow under wave forcing and the orbital horizontal and vertical velocities are significantly decreased by the vegetation.

More recently, Wang et al. (2016) studied the hydrodynamics due to waves and currents in the presence of vegetation. They showed that waves accelerate the flow velocity at the crest of the water surface, the turbulence intensity during the current-wave condition increases compared to current-only conditions and decreases due to the blocking effect of the vegetation.

The present work aims to collect new information about the interaction between seagrass and waves by means of an experimental investigation. Such new experiments extend the preliminary studies of Cavallaro et al. (2010) by carrying out new tests with several water levels and by also considering the blade flexibility in the analysis of results.

The paper is organized as follows. Section 2 presents the experimental setup. Section 3 shows the analysis related to the wave height dumping while Section 4 presents the results of the velocity attenuation inside the meadow. Concluding remarks are made in Section 5.

## 2. Experimental Setup

The experiments were carried out at the Hydraulics Laboratory of the University of Messina. The wave flume, shown in Fig. 1, is about 18.00 m long, 0.42 m wide and 0.80 m high. Regular waves are generated by means of a flap-type wavemaker, which is driven by a pneumatic system and is electronically controlled. Moreover, a gravel absorbing beach, composed of marble stones with a median diameter  $D_{50} = 3$  cm, is placed at the opposite side of the flume, with a slope equal to 1:4.

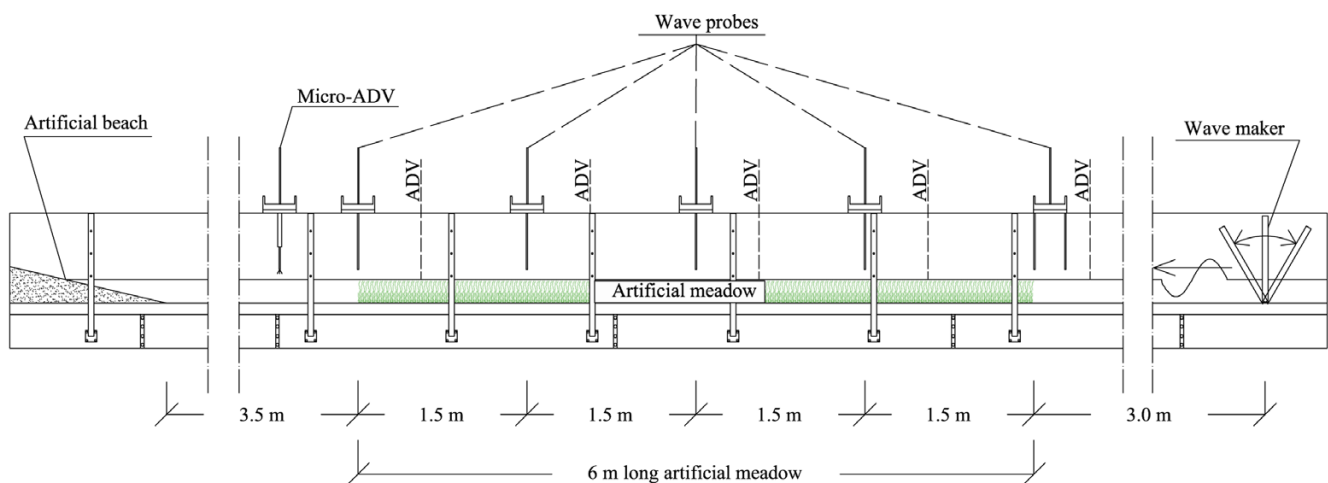


**Fig. 1.** Lateral view of the adopted experimental apparatus: wave channel with artificial meadow; the channel is equipped with an Acoustic Doppler Velocimeter (ADV) and wave probes

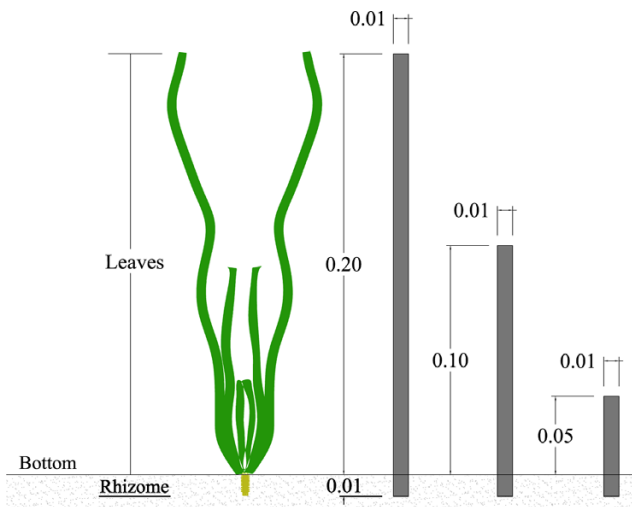


**Fig. 2.** Artificial plant used for the experiments: single stem made of 6 leaves (left), with three different lengths (right). All the dimensions are expressed in meters

The reference system is chosen in such a way that the  $x$  axis corresponds with the direction of wave propagation, and the  $z$  axis is vertical and points upward ( $z = 0$  at the bottom).

Inside the wave flume, a 6.0 m long synthetic meadow

was realized at a distance of 3.0 m from the wavemaker, such a length being enough to dissipate the evanescent standing waves generated by the wavemaker. Indeed, such waves are negligible two or three water depth away from the wavemaker (Dean and Dalrymple 1991). The meadow is composed of artificial plants realized with low density polyethylene. Each artificial stem is composed of six leaves with the same width, equal to 0.01 m, and three different heights: 0.05 m, 0.10 m, and 0.20 m (see Fig. 2). These plants are fixed to a metal plate in a regular grid with a density of 1,024 plants/m<sup>2</sup> (see Fig. 3). This plant configuration reproduces the *Posidonia Oceanica*, which is an endemic plant of the Mediterranean Sea. The polyethylene was chosen in order to reproduce the buoyancy and flexibility of real plants (see Cavallaro et al. 2010).

Five resistance wave gauges were placed across the meadow, at a mutual distance of 1.50 m. The wave gauge placed at the wavemaker side edge of the meadow was coupled with an additional gauge in order to estimate the wave reflection. Once collected from the wave gauges, the surface elevation data were post-processed in order to obtain the measured energy spectra, by using a Direct Fourier Transform (DFT) analysis. Then, the spectra of the incident and reflected waves

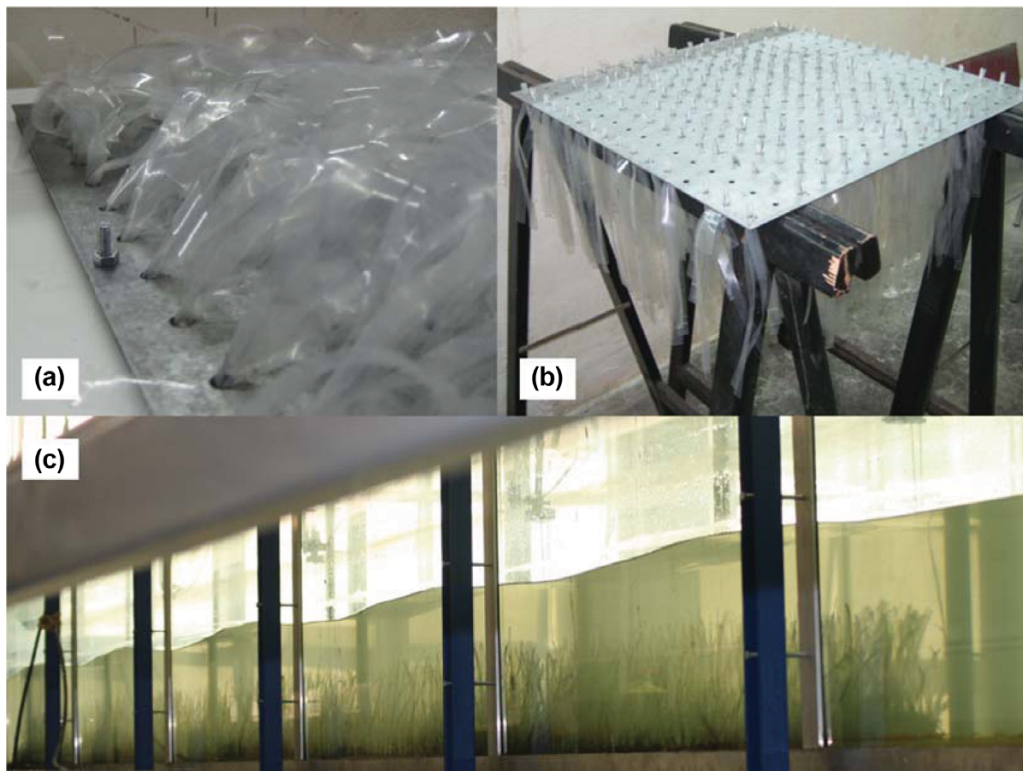


**Fig. 3.** Views of the tested artificial vegetation: (a) detail of the blades; (b) assembly of the model; (c) surface waves over the meadow

were calculated by applying the Goda and Suzuki (1976) method. The knowledge of such energy spectra allows for the estimation of both the incident and the reflected wave heights ( $H_i$  and  $H_r$ , respectively), and in turn of the reflection coefficient  $K_r = H_r/H_i$ . Such a coefficient falls within the range 0.10–0.15 for all the wave conditions which can be tested at the flume.

A Sontek Micro Acoustic Doppler Velocimeter (a 10 MHz ADV probe plus the ADVLab processor) was used to measure the three velocity components. The micro-ADV was located on a movable carriage, which allows the probe to be moved both horizontally and vertically. The sampling volume is a cylinder 9 mm high with a volume equal to 0.3 cm<sup>3</sup>, located 5 cm far from the transmitter. The adopted sampling frequency is 30 Hz. During the experiments, the water temperature measured in the tank is quite constant, in the range 19°–21°C, and therefore the value of the kinematic viscosity is assumed to be constant and equal to its value at 20°C, i.e.  $\nu = 1.00 \times 10^{-6}$  m<sup>2</sup>/s. The obtained velocity profiles refer to the lower part of the water column, since no measurement can be taken between the wave crest and the level 5 cm below the wave trough. The mean velocity profiles were obtained by positioning the ADV at a fixed point and by acquiring the velocity for at least 180 s.

The tests were carried out under regular waves characterized by heights in the range 0.020–0.135 m and periods in the range 0.6–1.6 s. Furthermore, the still water depth is in the range 0.29–0.45 m. It must be pointed out that wave periods longer than those indicated above cannot be reproduced without introducing too much disturbance, due to the limits imposed by the length of the wave flume.

### 3. Wave Height Reduction

#### Methodology

The presence of a meadow under progressive waves may cause energy reduction and wave height attenuation toward the direction of propagation. Such an effect is due to the mutual interaction between waves and leaves, which at the same time involves the movement of leaves and an increase of turbulence in comparison to the undisturbed orbital flow.

The approach adopted here for analysing the wave height reduction is that proposed by Dalrymple et al. (1984) and expanded upon by Mendez and Losada (2004). Such an approach is applicable to any kind of plant, under arbitrary water depth and vertical extent of the leaves over the water

column. All the unknown complex interactions between waves and plants are included in the drag coefficient  $C_D$ , which is assumed to be constant over the depth. That approach is valid for both rigid and flexible plants, since  $C_D$  can assume different values as a function of the flexibility of leaves.

The reduction of wave height  $H$  over the vegetation can be expressed as a function of the generic longitudinal distance  $x$  from the offshore boundary of the meadow:

$$K_v = \frac{H}{H_0} = \frac{1}{1 + \beta x} \quad (1)$$

where  $K_v$  is the damping coefficient;  $H_0$  is the incident wave height, registered at  $x = 0$ ;  $\beta$  is a parameter independent from  $x$  and related to the characteristics of both waves and meadow.

Dalrymple et al. (1984) derived  $\beta$  from the conservation of energy equation, by applying the linear wave theory. Similarly, Mendez and Losada (2004) obtained the following formula which is valid for monochromatic waves propagating over a horizontal bottom:

$$\beta = \frac{4}{9\pi} C_D b_v N H_0 k \frac{\sinh^3(k\alpha h) + 3\sinh(k\alpha h)}{[\sinh(2kh) + 2kh]\sinh(2kh)} \quad (2)$$

where  $b_v$  is the plant area per unit height of each vegetation leaf perpendicular to the horizontal flow velocity,  $N$  is the number of vegetation stems per unit horizontal area,  $k$  is the wave number,  $h$  is the water depth,  $\alpha = h_s/h$  is the relative plant height submergence ratio and  $h_s$  is the height of the leaves.

It is important to stress that the only dissipation term in Eq. 2 is due to the drag coefficient  $C_D$ , which contains all the neglected aspects in the interaction between waves and meadow: plant shape and flexibility, interaction between the leaves, length scale and amount of the turbulence induced by the meadow. Such neglected aspects should be taken into account in the choice of  $C_D$ .

A possible approach is to introduce several dimensionless parameters, which take into account the wave-meadow interaction phenomena not described in Eq. 2. Those parameters can be linked with  $C_D$  by means of empirical relations.

The parameter first adopted in the literature (see Kobayashi et al. 1993) is the Reynolds number defined as:

$$Re = \frac{b_v u_c}{\nu} \quad (3)$$

in which  $\nu$  is the kinematic viscosity and  $u_c$  is a characteristic

fluid velocity acting on the meadow, defined as the wave orbital velocity amplitude above the leaves. In particular, Mendez et al. (1999) and Koftis et al. (2013) suggest using the maximum velocity above the meadow, at its offshore edge:

$$u_c = \frac{\pi H_0 \cosh(k\alpha h)}{T \sinh(hk)} \quad (4)$$

Another parameter often related to  $C_D$  is the Keulegan-Carpenter number  $KC$  (see Mendez and Losada 2004; Bradley and Houser 2009; Sanchez-Gonzalez et al. 2011; Houser et al. 2015) which is the ratio of the length scale of oscillatory flow over the length scale of the vegetation:

$$KC = \frac{u_c T}{b_v} \quad (5)$$

Furthermore, a frequency parameter related to the interaction of a cylindrical element with an oscillatory flow can be applied (Sumer and Fredsoe 1997; Scandura et al. 2009):

$$\beta_w = \frac{Re}{KC} = \frac{b_v^2}{\nu T} \quad (6)$$

The above mentioned parameters do not take into account the flexibility of the leaves since the only parameter related to the leaves is the average width  $b_v$ . Therefore, another dimensionless group is needed which also considers the slenderness and the elasticity of the leaves. Luhar and Nepf (2011) proposed the use of the Cauchy number ( $Ca$ ), which is independent from  $C_D$  in oscillatory flows (see Luhar and Nepf 2016):

$$Ca = \frac{\rho b_b u_c^2 l^3}{EI} \quad (7)$$

where  $\rho$  is the fluid density,  $b_b$  is the leaf width,  $l$  is the length of the leaf,  $E$  is the modulus of elasticity,  $I$  is the second moment of area for the leaf cross-section;  $I = b_b t^3/12$  for rectangular cross-sections, where  $t$  is the thickness of the leaves.

The definition of the Cauchy number must be modified for the meadow with variable length of blades, since  $l$  is not unique. In particular, the relative occurrence  $p_i$  of each generic length  $l_i$  must be considered. In this specific case, the lengths of blades are distributed uniformly among three different values:  $h_c$ ,  $h_c/2$  and  $h_c/4$ . Therefore,  $p_i$  is always equal to  $1/3$  and term  $l^3$  in Eq. 7 becomes:

$$l^3 = \sum_{i=1}^n p_i l_i^3 = \frac{h_c^3}{3} \left( 1 + \frac{1}{8} + \frac{1}{64} \right) \quad (8)$$

Houser et al. (2015) proposed a parameter  $\lambda$  slightly different

from  $Ca$  which is proportional to the rigidity of the blades rather than to their flexibility. The same variables are used in those parameters, thus they can be related under the assumption of blades with rectangular cross-sections:

$$\lambda = \frac{Et^3}{l^3 u_c^2} = \frac{12\rho}{Ca} \quad (9)$$

Such an equation highlights that  $\lambda$  and  $Ca$  are interchangeable for a given fluid, i.e. for fixed  $\rho$ . Only the Cauchy number is used hereinafter, since it is dimensionless and assures a better generalization of the experimental outcomes.

### Analysis of results

Wave heights registered during the experiments are used here for the estimation of the wave damping related parameter  $\beta$ . Such a parameter is independent from the longitudinal abscissa inside the meadow but it is related to the meadow characteristics and to the wave conditions.

For each test,  $\beta$  is obtained by means of a best fit of Eq. 1 applied to the observed wave heights. The capability of that relation in interpreting wave damping is estimated by means of the normalized root mean square error of the coefficient  $K_v$ , defined as follows:

$$NRMSD(K_v) = \frac{1}{K_{v,max} - K_{v,min}} \sqrt{\frac{\sum_{i=1}^n (\widehat{K}_v - K_v)^2}{n}} \quad (10)$$

where  $K_{v,max}$  and  $K_{v,min}$  are the maximum and minimum values of the damping coefficient respectively;  $K_v$  is the value estimated from the measurements;  $\widehat{K}_v$  is the value predicted by means of the best fit for Eq. 1;  $n$  is the number of sections over the meadow at which wave height has been measured. In the present experiments  $n = 5$  since there are 3 wave gauges inside the meadow and 2 at its edge.

In order to assess the reliability of the acquired data, some preliminary analyses are performed. First, the coefficient  $\beta$  is estimated also by means of a simpler and more straightforward procedure, which takes into account only the wave heights at the edge of the meadow. In particular,  $K_v$  and  $x$  are related only to the shoreward edge of the meadow and a unique value of  $\beta$  can be obtained from Eq. 1. That methodology is quite crude. Nevertheless, its results can be compared to those obtained by means of the best fit inside the meadow, in order to validate the adopted relationship for estimating the wave height reduction (i.e. Eq. 1). The values of  $\beta$  obtained by means of the two methods are used, together with the incident wave characteristics, for estimating  $C_D$  for all the

tests carried out.

In order to assess the reliability of Eq. 1 in estimating wave dumping, a comparison is reported in Fig. 4a between the results obtained from wave heights along the meadow and at its edge.

Two tests show the greatest errors, with values of  $NRMSD(K_v) \geq 0.25$ . The same tests highlight also a mismatch between values of  $C_D$  estimated with the two methods described above, thus they have been excluded. Symmetrically, the tests with lower errors of  $K_v$  are those in which the two methodologies are more in accordance. Such a result

confirms the reliability of the adopted formulation also when only data at the edge of the meadow are available, as in the experiments carried out previously by Cavallaro et al. (2010) with the same artificial plants. Therefore, those experiments have also been taken into account in the present work.

A further preliminary analysis of data was carried out in order to compare the incident wave characteristics with the breaking limit value  $H_b$  proposed by Miche (1944):

$$\frac{H_b}{L} = 0.142 \tanh\left(\frac{2\pi h}{L}\right) \tag{11}$$

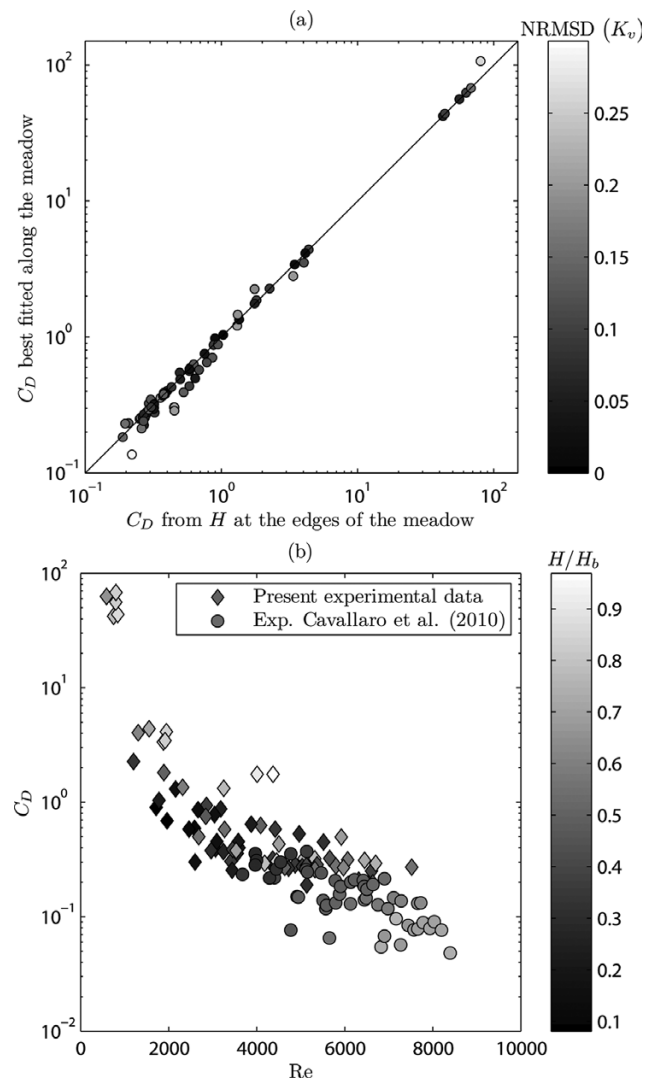
where  $L$  is the wave length obtained from the dispersion relation on the basis of the wave period  $T$  and the still water depth  $h$ .

Fig. 4b shows  $C_D$  as a function of  $Re$  and breaking ratio  $H/H_b$ . Obviously, such a ratio is always lower than 1 since higher values would be physically impossible due to the activation of the wave breaking phenomenon. Nevertheless, values of  $H/H_b$  close to 1 highlight the presence of unstable near-breaking conditions or breaking phenomena underway. In those cases, wave dumping related coefficients ( $\beta$  and  $C_D$ ) can be amplified independently from the meadow. In order to identify such conditions, a safe limit of  $H/H_b$  must be considered.

Fig. 4b shows that two tests furnish values of  $C_D$  and  $Re$  which are not in agreement with the trend of the remaining data and show amplified values of  $C_D$ . Such tests are slightly below the Miche's breaking limit since  $H/H_b > 0.85$ . Thus, they can be affected by breaking phenomenon and are excluded from the following analysis.

The methodology adopted for wave dumping estimation is valid for linear waves. Its limit is tested here by considering the effect of the nonlinear parameter  $L/h$  on the values of  $\beta$  obtained alternatively at the edge of the meadow and with the best fit along the meadow. Fig. 5 shows that the two adopted methodologies provide similar values for  $L/h < 7$ . Such a threshold value corresponds to the shallow water limit proposed by Dingemans (1997): nonlinear models can be considered reliable above such a value. For nonlinear waves (i.e.  $L/h \geq 7$ ), Fig. 5 shows a deviation from the bisecting line. Therefore, the coefficients  $\beta$  obtained from the wave heights at the edges of the meadow are slightly overestimated in comparison to those obtained by means of the best fitting procedure.

Such a result does not influence the reliability of the adopted methodology if best fitted data are taken into



**Fig. 4.** Data analysis for the recognition of outliers: (a) comparison between drag coefficient  $C_D$  interpolated and at the edges of the meadow, grey intensity is related to the normalized root mean square error of  $K_v$ ; (b)  $C_D$  as a function of Reynolds number  $Re$  for present and Cavallaro et al. (2010) experiments, gray intensity is related to wave breaking ratio  $H/H_b$

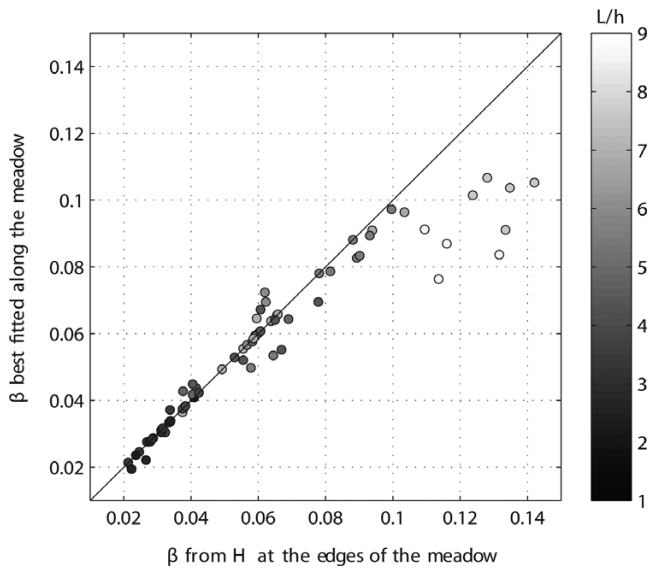


**Fig. 5.** Comparison between coefficient  $\beta$  obtained as an interpolation over the horizontal position and at the edges of the meadow. The gray scale is a function of  $L/h$

account. Furthermore, the highlighted differences in  $\beta$  are less evident in the drag coefficient  $C_D$ , as shown in Fig. 4.

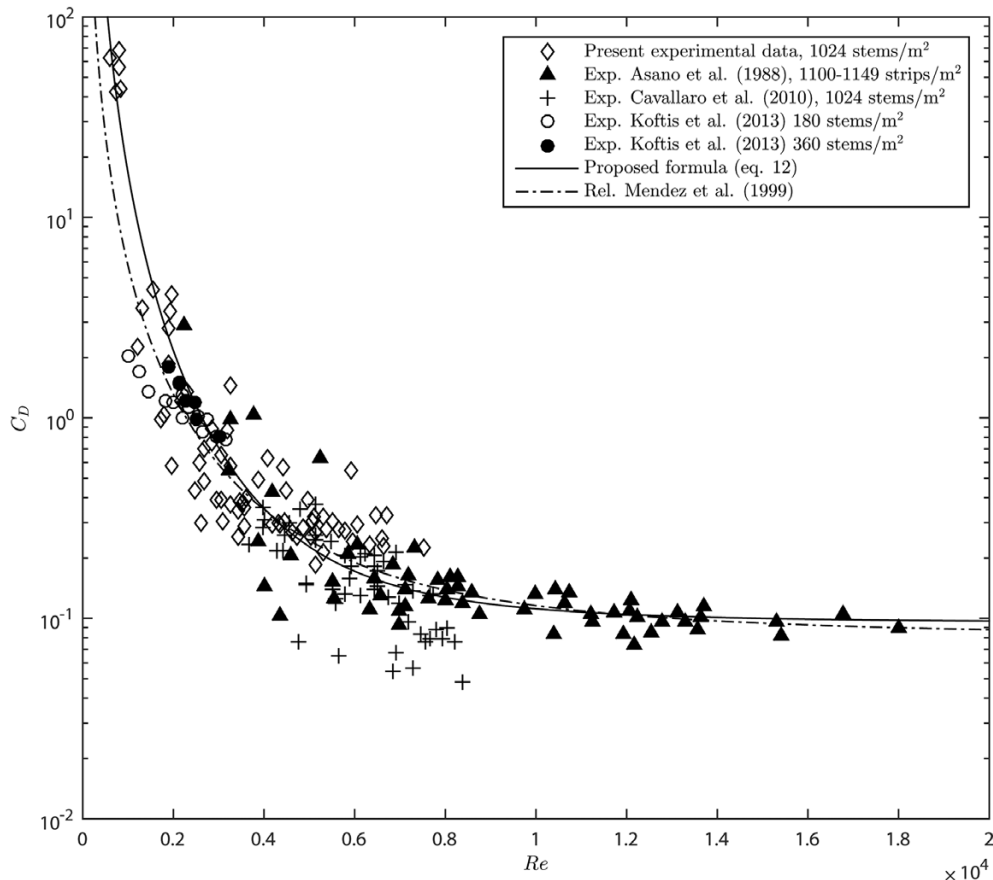
The central role of  $C_D$  on wave-meadow interaction is confirmed by the number of past studies which have taken into account such a coefficient. The results obtained from the present tests are compared with experiments carried out in fairly similar conditions by Asano et al. (1988), Cavallaro et al. (2010) and Koftis et al. (2013).

Fig. 6 shows  $C_D$  as a function of  $Re$  for present and past experiments, from which a decreasing trend can be noted. A kind of formula which can fit those data is that proposed by Kobayashi et al. (1993):

$$C_D = \left(\frac{a}{Re}\right)^b + c \tag{12}$$

where the coefficients  $a$ ,  $b$  and  $c$  can be calibrated by means of experimental data. Table 1 summarizes the values of such coefficients in the formula proposed here and in similar relations from the literature.

The proposed formula is compared in Fig. 6 with that proposed by Mendez et al. (1999), which was calibrated on the basis of experiments of Asano et al. (1988). Both formulas are able to describe fairly accurately the experimental data



**Fig. 6.** Variation in drag coefficient  $C_D$  as a function of the Reynolds number  $Re$ ; experimental data and empirical relations

**Table 1.** Values of coefficients *a*, *b* and *c* of Eq. 12, proposed in the literature and in the present study

Formula	a	b	c
Kobayashi et al. (1993)	2200	2.40	0.080
Mendez et al. (1999)	2200	2.20	0.080
Cavallaro et al. (2010)	2100	1.70	0
Koftis et al. (2013)	2400	0.77	0
Proposed formula	2550	3.05	0.095

for  $Re > 5000$ , i.e. high Reynolds numbers. For  $Re < 4000$ , the proposed formulation provides a better match with the present experiments and with the experiments carried out by Koftis et al. (2013) with a density of the meadow equal to 360 stems/m<sup>2</sup>.

Flexibility of the blades is a common factor in the tests presented here and in the literature experiments cited above. The relationship between  $C_D$  and the Cauchy number  $Ca$  is shown in Fig. 7 for all those tests. Such results do not highlight a clear trend, above all when the tests of Asano et al. (1988) are considered. A possible reason is that the latter tests are related to very wide blades (i.e.  $b_b = 5.2$  cm) which may

cause stronger drag forces in comparison to the blades tested in all the other experiments taken into account, which have  $b_b = 1$  cm.

The formula proposed by Houser et al. (2015) is expressed as a function of the flexibility parameter  $\lambda$ , which can be related to  $Ca$  by considering Eq. 9, so becoming:

$$C_D = 0.0133\lambda^{0.86} = \left(\frac{79}{Ca}\right)^{0.86} \tag{13}$$

Such a formula represents in Fig. 7 a lower boundary for the values of  $C_D$  considered here. That boundary is crossed by the large scale experiments of Koftis et al. (2013) carried out with low density vegetation, i.e. 180 stems/m<sup>2</sup>. The outcomes of the present experiments are far from the results of Eq. 13 for the lowest values of the Cauchy number, i.e.  $Ca < 100$ . If the experiments of Asano et al. (1988) are excluded, a better agreement is found for  $Ca > 100$ .

A high variability of  $C_D$  is highlighted in both Figs. 6 and 7, as a function of  $Re$  and  $Ca$  respectively. Therefore, the wave-meadow interactions must be investigated more in depth, in order to understand the rationale behind such a variability.

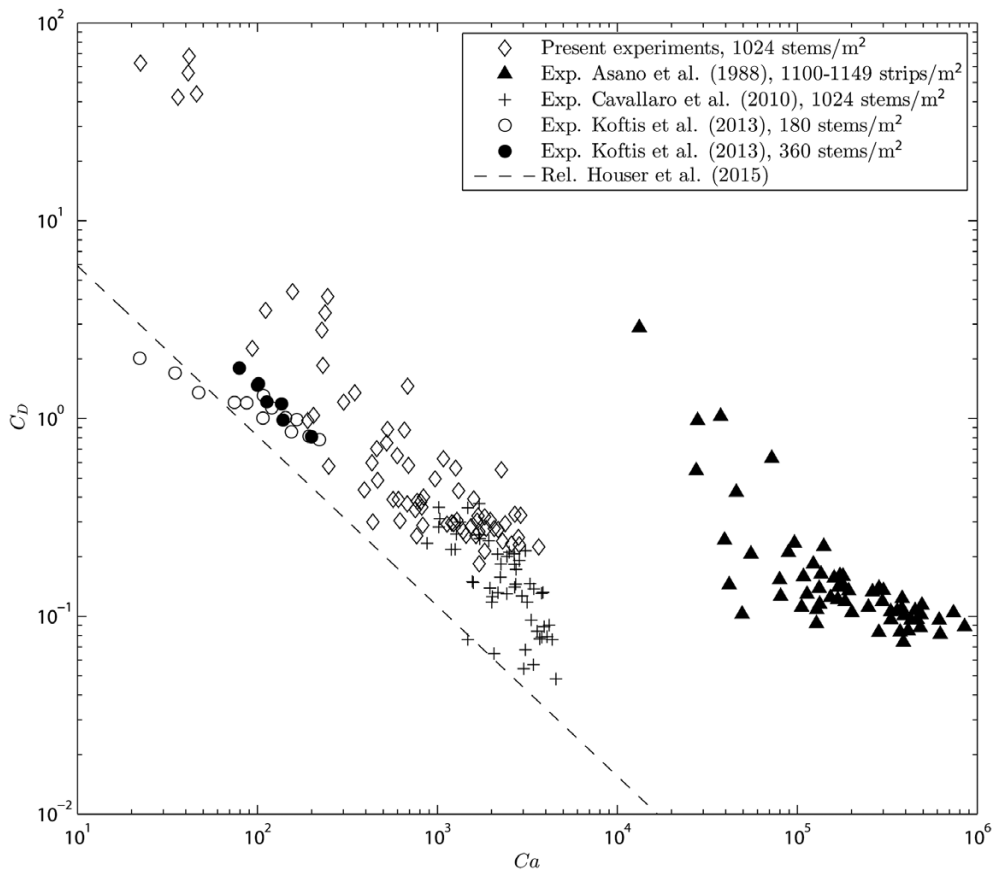


**Fig. 7.** Drag coefficient  $C_D$  as a function of the Cauchy number  $Ca$ , which takes into account blade flexibility

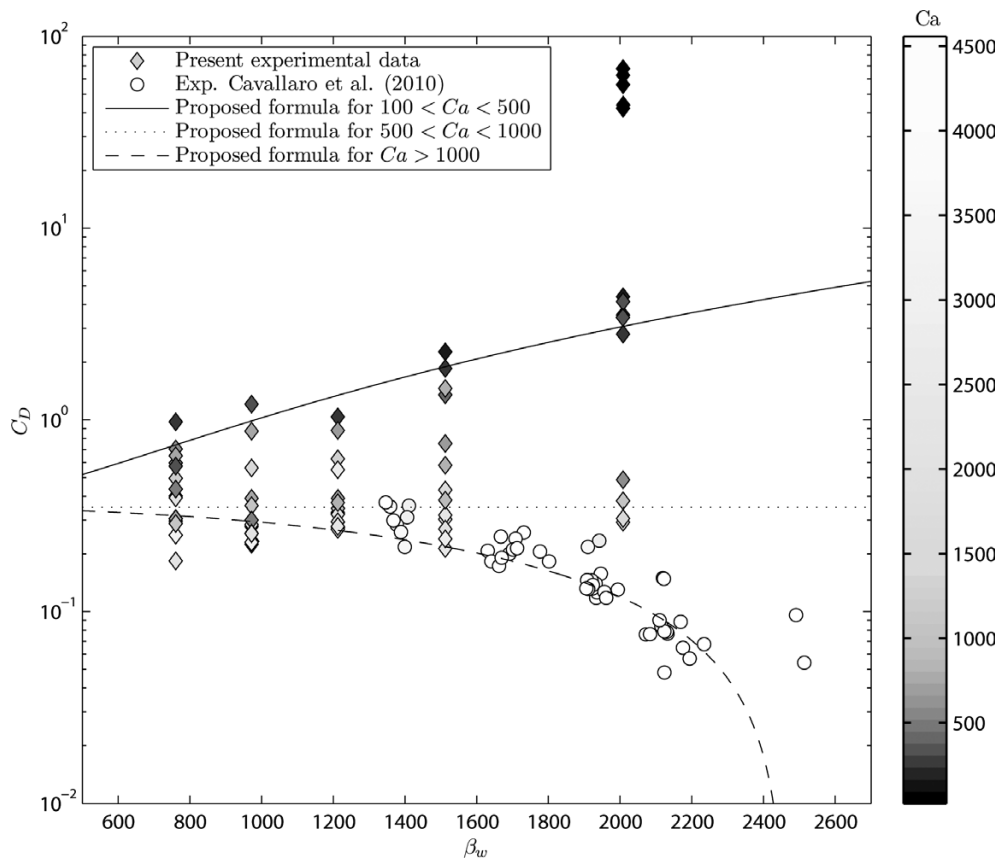


**Fig. 8.** Drag coefficient  $C_D$  as a function of the frequency parameter  $\beta_w = b_v^2/(vT)$ , for the present experiments and for the available data of Cavallaro et al. (2010). Grey intensity is proportional to Cauchy number  $Ca$ ; the trend lines are shown for three ranges of  $Ca$

A new approach is proposed here which takes into account  $\beta_w$ , i.e. the ratio between Reynolds and Keulegan-Carpenter numbers. Such a variable is called ‘frequency parameter’ since it is related to the wave period (see Eq. 6). That parameter is considered in Fig. 8 together with  $Ca$  in order to investigate their simultaneous effect on  $C_D$ . The results are obtained for the present experiments and for the rehashed data of Cavallaro et al. (2010) and show different trends for the same frequency parameter as a function of  $Ca$ : (i)  $C_D$  increases with  $\beta_w$  for small Cauchy numbers, i.e. for light-gray symbols in Fig. 8; (ii)  $C_D$  decreases with  $\beta_w$  for high values of  $Ca$  (dark-gray symbols). Between these trends, a transition region is present for which the drag coefficient is fairly constant.

The rationale behind such a dramatic change in trend can be found in the coupled effect of the bending of blades and of wave frequency. The blades are close to the bottom when  $Ca > 1000$ , so the actual height of the meadow is lower than the length of the leaves, and the water column in which the flow interacts with the vegetation is smaller. In these conditions,

the increase of frequency parameter  $\beta_w$  corresponds to lower values of the wave period which induce a reduction of orbital velocities inside the meadow, on the basis of the linear wave theory. On the whole, the reduction of inside-meadow velocities and the increase in bending of the meadow itself cause a reduction of interaction between waves and vegetation, in terms of drag coefficient. Conversely, lower values of the Cauchy number (i.e.  $Ca < 500$ ) mean that the leaves are more rigid against the flow. If the frequency parameter increases in such conditions, the reduction of the wave period  $T$  causes a further tendency of the leaves to remain straight since the flow acts for a smaller time (equal to  $T/2$ ) in one direction, after which it reverses. Essentially, the straighter the leaves, the greater the drag force. For the present experimental data, that effect is strongly amplified for very low values of orbital velocities, i.e. for  $Re < 1000$  and  $Ca < 100$ . In such conditions, viscous forces dominate the interaction between waves and meadow and  $C_D > 30$ . It is important to stress that the latter conditions correspond to very low wave heights, which do not appreciably affect the coastal hydro-morphodynamics.

**Table 2.** Proposed values of coefficient  $d$  in Eq. 14 for classes of the Cauchy number  $Ca$

Range	$d$
$100 < Ca < 500$	$6.8 \times 10^{-7}$
$500 < Ca < 1000$	0
$Ca > 1000$	$-5.8 \times 10^{-8}$

In order to highlight the different behaviours of  $C_D$  discussed above, three trend lines are shown in Fig. 8, which have all the following form:

$$C_D = d(\beta_w)^2 + 0.35 \tag{14}$$

the coefficient  $d$  moves from positive to negative values with increasing  $Ca$ , as summarized in Table 2.

The lowest values of the Cauchy number ( $Ca < 100$ ) have been excluded from that analysis since those data are available only for high values of  $\beta_w$ . However, the results obtained by means of  $Re$  from Eq. 12 are already satisfactory in those conditions, since such a range of  $Ca$  corresponds to the maximum of  $C_D$  in Fig. 6 which is fitted adequately by means of that formula.

It is worth pointing out that Eq. 14 differs from Eq. 12 since  $C_D(\beta_w)$  may have an increasing trend (for  $Ca < 500$ ).

Conversely  $C_D(Re)$  is always decreasing. Such a different behaviour is due to the fact that  $\beta_w$  is a function of the stem width and of the wave period, whereas  $Re$  is also dependent on the wave height.

### 4. Velocity Attenuation

According to the linear wave theory (Dean and Dalrymple 1991), the horizontal and vertical velocity under a progressive wave propagating over a flat bottom is given by

$$u = \frac{\sigma H \cosh(kz)}{2 \sinh(kh)} \cos(kx - \sigma t) \tag{15}$$

$$w = \frac{\sigma H \sinh(kz)}{2 \sinh(kh)} \sin(kx - \sigma t) \tag{16}$$

where  $\sigma = 2\pi/T$  is the wave radian frequency. It is worth recalling here that the vertical coordinate  $z$  is measured from the bottom of the flume. Such a description of the flow under progressive waves is obtained by assuming perfectly inviscid irrotational motion and by neglecting the nonlinear term in the Navier-Stokes equations.

The result of these assumptions is a flow with zero mean velocity. However, the observation of the flow field under a

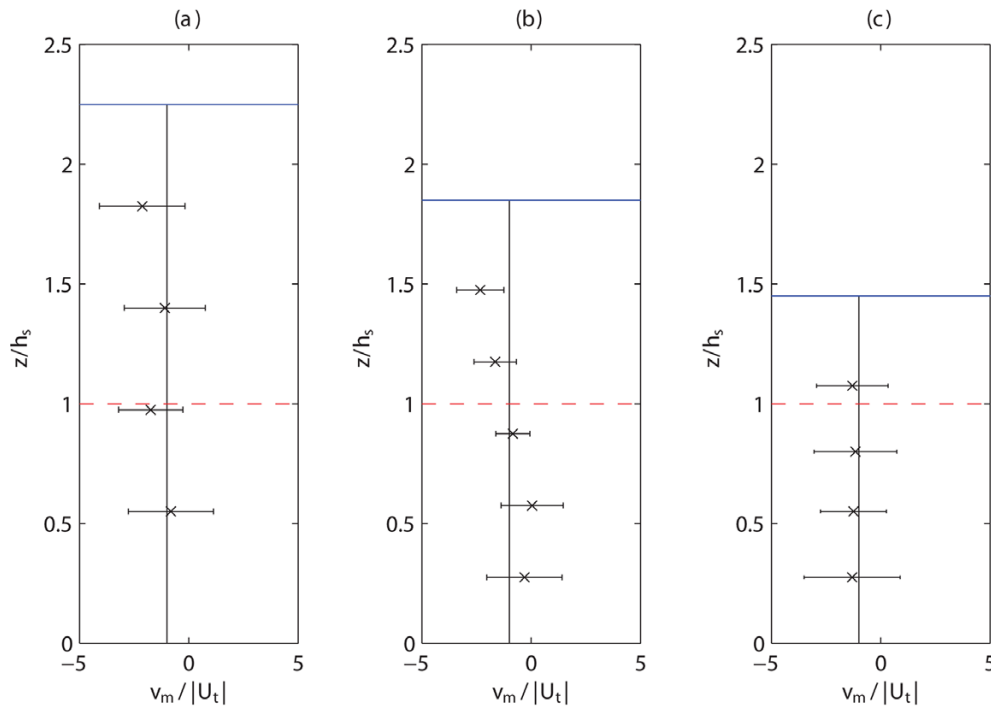


**Fig. 9.** Profiles of average velocities  $v_m$  over the mass transport velocity from linear theory  $|U_t|$ : (a) high water depth condition; (b) intermediate water depth; (c) small water depth. Dashed line is the maximum height of the meadow

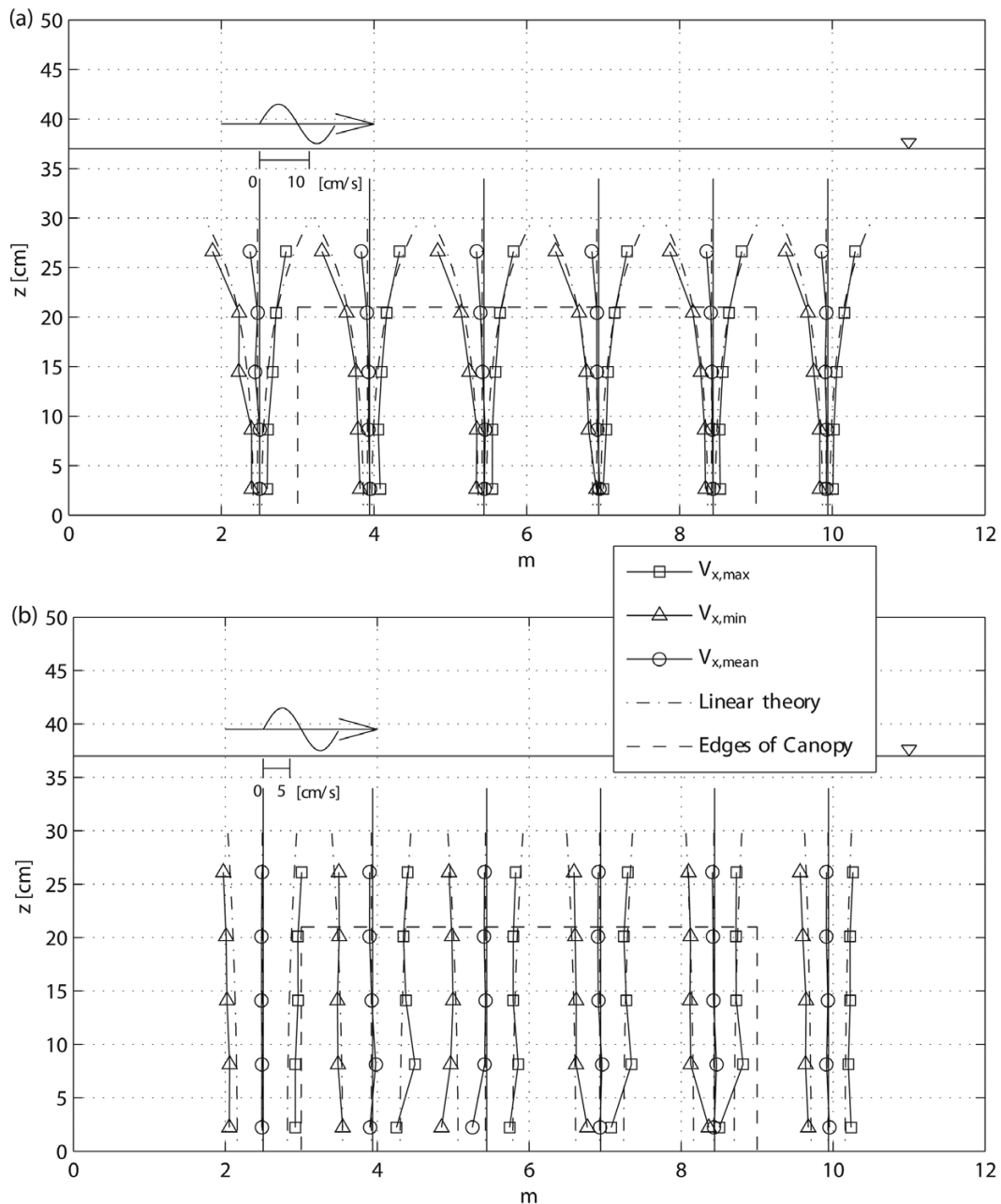


**Fig. 10.** Horizontal velocity profiles measured and predicted from the linear wave theory for two tests carried out with still water depth  $h = 0.37$  m: (a) incident waves having  $H = 0.04$  m,  $T = 0.6$  s; (b) incident waves having  $H = 0.04$  m,  $T = 1.6$  s

progressive wave shows non-zero values for the mean horizontal velocity. Such a mass transport is generated by the nonlinear effect of wave propagation (Dean and Dalrymple 1991) and by the effect of the flow viscosity for laminar flow (Longuet-Higgins 1953) or turbulence asymmetry near the bottom (Scandura 2007; Cavallaro et al. 2011).

More particularly, as first indicated by Starr (1947) the mass transport in the direction of wave propagation due to

the nonlinear effect of wave propagation (the so called Stokes drift) is equal to:

$$M = \frac{E}{C} \tag{17}$$

where  $E = 1/8\rho gH^2$  is the wave total average energy per unit surface area,  $C = L/T$  is the wave celerity,  $\rho$  is the water density,  $g$  is the gravitational acceleration,  $H$  is the wave height,  $L$  is

the wavelength, and  $T$  is the wave period. Such a mass transport is concentrated in the region between the crest and the trough of a wave (Dean and Dalrymple 1991).

In a wave tank such a mass transport, co-directional with the wave direction, must be balanced by a mean current directed toward the wavemaker. This return current modifies the flow above and inside the meadow. An estimate of that return depth-averaged velocity could be obtained by means of the following relation:

$$U_t = \frac{M}{\rho h} \tag{18}$$

In the presence of a meadow, Luhar et al. (2010) found that a mean current in the direction of wave propagation is generated within the meadow due to the nonlinear interaction with the oscillatory velocity. An estimate for the mean current generated within the meadow is:

$$U_{c,m} = \sqrt{\frac{4 C_{Dw} k^3}{3\pi C_{Dc} \sigma} u_{w,m}^3} \tag{19}$$

where  $C_{Dw}$  and  $C_{Dc}$  are respectively steady and time-varying components of the drag coefficients, and  $u_{w,m}$  is the magnitude of the in-meadow oscillatory flow.

Luhar et al. (2010) found that the impact of the return current, due to both the Stokes drift and the presence of the meadows, is negligible within the meadow. However, the present results show that the return current inside the meadow cannot be neglected and its value is greater than the mean current generated by the presence of the meadow (see Fig. 9). Indeed, the time-averaged velocities inside the meadow show negative values and their mean value over the depth is close to  $U_t$ .

Regarding the velocity structure, Koftis et al. (2013) reported that inside the meadow the orbital horizontal and vertical velocities are significantly decreased. During the present experiments six velocity profiles were detected: two outside the meadows and four inside the meadow. The results of the present experiments show a strong correlation between the wave height dumping and the velocity dumping due to the presence of the meadow.

As shown in Fig. 10 for the two tests, the velocity profiles along the meadow are close to those evaluated by the linear wave theory in which the local wave height is adopted. Such a local height is defined as that evaluated at the same section where the velocity profile is registered. Therefore, the velocity provided by the linear wave theory is coupled with

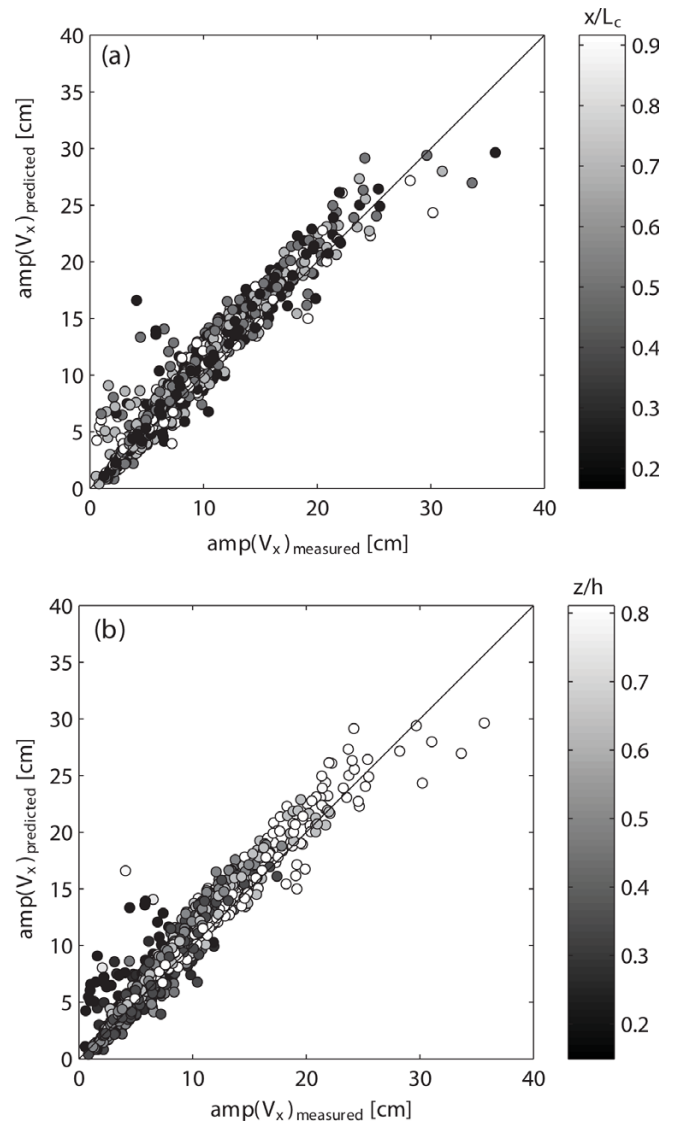


**Fig. 11.** Orbital velocity amplitudes measured and predicted from the linear wave theory

the return current generated by the Stokes drift. The same analysis was carried out for all the tests.

Fig. 11 shows the amplitude of the registered orbital horizontal velocities versus the values of the corresponding variable evaluated by means of the linear wave theory. Such a representation demonstrates that the correlation between the amplitude of the orbital velocity and the local wave height is substantially independent from the vertical and horizontal position along the meadow.

### 5. Conclusions

The interaction between a meadow and surface waves

involves complex hydrodynamics related to both incident wave conditions and flexibility of the leaves. By means of physical modelling, two main effects of such an interaction are considered in the present work: wave height reduction and velocity profile modification in comparison to the linear wave theory.

The experiments were carried out for a dense meadow composed of polyethylene blades, in which flexibility played a key role.

The analysis of the drag coefficient as a function of the Reynolds number confirms a decreasing trend widely investigated in the literature by means of a power law. The relevant number of experiments, carried out in the present work in a wide range of  $Re$ , further improves that existing formula with a focus on flexible leaves with high density.

Leaf flexibility effect on the wave dumping was analysed by a direct comparison between the Cauchy number and drag coefficient. An existing formulation is shown to represent a lower limit for the test carried out. Nevertheless, the values of  $C_D$  are dramatically underestimated by that formulation, especially for small values of  $Ca$ .

Furthermore, a coupled analysis of the results is performed as a function of the Cauchy number and frequency parameter. Such an analysis highlights the presence of very different behaviours for three classes of  $Ca$ : (i)  $C_D$  increases with the wave frequency for small values of the Cauchy number, i.e. for  $Ca < 500$ ; (ii)  $C_D$  assumes a nearly constant value for  $500 < Ca < 1000$ ; (iii)  $C_D$  decreases as a function of  $\beta_w$  for highly flexible leaves ( $Ca > 1000$ ). Therefore, the change of flexibility modifies the response of the leaves to the waves. In particular, the leaves have a small tendency to bend for small values  $Ca$ . In these conditions, an increase in wave frequency causes a reduction of the period in which the flows act in one direction. Thus, the leaves are straight for a longer time and the drag coefficient increases dramatically. On the other hand, the leaves are unable to stay vertical for very large values of  $Ca$  and are always bent toward the bottom, independently from the wave conditions. In such cases, an increase in wave frequency causes a reduction of the orbital waves near to the bottom and of the interactions between waves and leaves.

A reduction of wave height is expected to cause a decrease in orbital velocity. The comparison of the registered amplitude of waves inside the meadow with the values predicted by the nonlinear theory have a fairly good match, if the dumped wave height is used. Therefore, the amplitude of orbital velocity does not highlight a clear variation along the water depth due

to the presence of the seagrass and its reduction is mainly related to the horizontal position along the seagrass.

Furthermore, the mean velocities inside the meadow are lower than those evaluated above the leaves. Such behaviour is probably due to the current generated inside the meadow due to the interaction between the leaves and the oscillatory velocity.

## Acknowledgements

This work has been partly funded by the EU funded project HYDRALAB PLUS (proposal number 64110), by the project “NEWS - Nearshore hazard monitoring and Early Warning System” (code C1-3.2-60) in the framework of the programme INTERREG V-A Italia Malta 2014-2020, and by University of Catania funded project “Interazione onde-correnti nella regione costiera (INOCS)”.

## References

- Asano T, Tsutsui S, Sakai T (1988) Wave damping characteristics due to seaweed. In: Proceedings of 35th coastal engineering conference in Japan, Japan Society of Civil Engineers (JSCE), pp 138–142 (in Japanese)
- Bouma TJ, De Vries MB, Low E, Peralta G, Tnczos IC, van de Koppel J, Herman PMJ (2005) Trade-offs related to ecosystem engineering: a case study on stiffness of emerging macrophytes. *Ecology* **86**(8):2187–2199. doi:10.1890/04-1588
- Bradley K, Houser C (2009) Relative velocity of seagrass blades: implications for wave attenuation in low-energy environments. *J Geophys Res-Earth* **114**(F1). doi:10.1029/2007JF000951
- Carpenter SR, Lodge DM (1986) Effects of submersed macrophytes on ecosystem processes. *Aquat Bot* **26**:341–370. doi:10.1016/0304-3770(86)90031-8
- Cavallaro L, Lo Re C, Paratore G, Viviano A, Foti E (2010) Response of *Posidonia Oceanica* to wave motion in shallow-waters - preliminary experimental results. In: Proceedings of 32nd Conference on Coastal Engineering (Shanghai, China), pp 49–59
- Cavallaro L, Scandura P, Foti E (2011) Turbulence-induced steady streaming in an oscillating boundary layer: on the reliability of turbulence closure models. *Coast Eng* **58**(4):290–304
- Dalrymple RA, Kirby JT, Hwang PA (1984) Wave diffraction due to areas of energy dissipation. *J Waterw Port Coast* **110**(1):67–79. doi:10.1061/(ASCE)0733-950X(1984)110:1(67)
- Dean RG, Dalrymple RA (1991) *Water wave mechanics for engineers and scientists*. World Scientific, Singapore, 368 p
- Dingemans M (1997) *Wave propagation over uneven bottoms*. Advanced Series on Ocean Engineering 13, World Scientific, Singapore, 700 p

- Goda Y, Suzuki T (1976) Estimation of incident and reflected waves in random wave experiments. In: Proceedings of 15th Conference on Coastal Engineering, Honolulu, Hawaii, pp 828–845
- Houser C, Trimble S, Morales B (2015) Influence of blade flexibility on the drag coefficient of aquatic vegetation. *Estuar Coast* **38**(2):569–577
- John BM, Shirlal KG, Rao S, Rajasekaran C (2016) Effect of artificial seagrass on wave attenuation and wave run-up. *Int J Ocean Clim Sys* **7**(1):14–19. doi:10.1177/1759313115623163
- Kobayashi N, Raichle AW, Asano T (1993) Wave attenuation by vegetation. *J Waterw Port C* **119**(1):30–48. doi:10.1061/(ASCE)0733-950X(1993)119:1(30)
- Koch EW, Sanford LP, Chen SN, Shafer DJ, Mckee SJ (2006) Waves in seagrass systems: review and technical recommendations. US Army Corps of Engineers, ERDC TR-06-15, 92 p
- Koftis T, Prinos P, Stratigaki V (2013) Wave damping over artificial *posidonia oceanica* meadow: a large-scale experimental study. *Coast Eng* **73**:71–83. doi:10.1016/j.coastaleng.2012.10.007
- Lakshmanan N, Kantharaj M, Sundar V (2012) The effects of flexible vegetation on forces with a keulegan-carpenter number in relation to structures due to long waves. *J Mar Sci App* **11**(1):24–33. doi:10.1007/s11804-012-1102-9
- Longuet-Higgins MS (1953) Mass transport in water waves. *Philos T R Soc A* **245**(903):535–581. doi:10.1098/rsta.1953.0006
- Lowe RJ, Koseff JR, Monismith SG (2005) Oscillatory flow through submerged canopies: 1. velocity structure. *J Geophys Res-Oceans* **110**(10):1–17
- Luhar M, Nepf H (2016) Wave-induced dynamics of flexible blades. *J Fluid Struct* **61**:20–41. doi:10.1016/j.jfluidstructs.2015.11.007
- Luhar M, Nepf HM (2011) Flow-induced reconfiguration of buoyant and flexible aquatic vegetation. *Limnol Oceanogr* **56**(6):2003–2017. doi:10.4319/lo.2011.56.6.2003
- Luhar M, Coutu S, Infantes E, Fox S, Nepf H (2010) Wave-induced velocities inside a model seagrass bed. *J Geophys Res-Oceans* **115**(C12):C12005. doi:10.1029/2010JC006345
- Luhar M, Infantes E, Orfila A, Terrados J, Nepf HM (2013) Field observations of wave-induced streaming through a submerged seagrass (*posidonia oceanica*) meadow. *J Geophys Res-Oceans* **118**(4):1955–1968
- Mendez FJ, Losada IJ (2004) An empirical model to estimate the propagation of random breaking and nonbreaking waves over vegetation fields. *Coast Eng* **51**(2):103–118. doi:10.1016/j.coastaleng.2003.11.003
- Mendez FJ, Losada IJ, Losada MA (1999) Hydrodynamics induced by wind waves in a vegetation field. *J Geophys Res-Oceans* **104**(C8):18383–18396. doi:10.1029/1999JC900119
- Miche R (1944) Mouvements ondulatoires de la mer en profondeur constante ou décroissante. *Annales des Ponts et Chaussées* **114**:25–78, 131–164, 270–292, 369–406 (in French)
- Peralta G, Brun FG, Prez-Llorns JL, Bouma TJ (2006) Direct effects of current velocity on the growth, morphometry and architecture of seagrasses: a case study on *zostera noltii*. *Mar Ecol-Prog Ser* **327**:135–142
- Sanchez-Gonzalez JF, Sanchez-Rojas V, Memos CD (2011) Wave attenuation due to *posidonia oceanica* meadows. *J Hydraul Res* **49**(4):503–514. doi:10.1080/00221686.2011.552464
- Scandura P (2007) Steady streaming in a turbulent oscillating boundary layer. *J Fluid Mech* **571**:265–280
- Scandura P, Armenio V, Foti E (2009) Numerical investigation of the oscillatory flow around a circular cylinder close to a wall at moderate Keulegan-Carpenter and low Reynolds numbers. *J Fluid Mech* **627**:259–290. doi:10.1017/S0022112009006016
- Starr VP (1947) A momentum integral for surface waves in deep water. *J Mar Res* **6**(2):126–135
- Sumer B, Fredsoe J (1997) Hydrodynamics around cylindrical structures. World Scientific, Singapore, 530 p
- Wang X, Xie W, Zhang D, He Q (2016) Wave and vegetation effects on flow and suspended sediment characteristics: a flume study. *Estuar Coast Shelf S* **182**:1–11. doi:10.1016/j.ecss.2016.09.009